AIP Applied Physics Letters

Plasmonic coupling of SiO2–Ag “post-cap” nanostructures and silver film for surface enhanced Raman scattering

Hsin-Yu Wu and Brian T. Cunningham

Citation: Appl. Phys. Lett. **98**, 153103 (2011); doi: 10.1063/1.3555342
View online: http://dx.doi.org/10.1063/1.3555342
View Table of Contents: http://apl.aip.org/resource/1/APPLAB/v98/i15
Published by the American Institute of Physics.

Plasmonic coupling of SiO_2–Ag "post-cap" nanostructures and silver film for surface enhanced Raman scattering

Hsin-Yu Wu[1] and Brian T. Cunningham[1,2,a)]
[1]*Department of Electrical and Computer Engineering, University of Illinois at Urbana-Champaign, Urbana, Illinois 61801, USA*
[2]*Department of Bioengineering, University of Illinois at Urbana-Champaign, Urbana, Illinois 61801, USA*

(Received 13 December 2010; accepted 24 January 2011; published online 11 April 2011)

We demonstrate a surface enhanced Raman scattering (SERS) substrate consisting of SiO_2–Ag "post-cap" nanostructures with an underlying silver film fabricated by the glancing angle deposition technique. Electromagnetic simulations predict that SERS enhancement is strongly polarization-dependent, consistent with experimental measurements. Optimized coupling between Ag cap nanoparticles and the underlying silver film can be achieved by controlling the thickness of SiO_2 post sandwiched between them to significantly enhance local electric-field intensity and to increase the density of electromagnetic hot spots. A maximum SERS enhancement factor of 2.38×10^9 within the hot spot region is demonstrated, providing sufficient sensitivity for many important applications. © *2011 American Institute of Physics*. [doi:10.1063/1.3555342]

Surface enhanced Raman spectroscopy (SERS) is a powerful method for increasing the cross section of Raman scattering, allowing for sensitive and selective detection of low concentration chemical and biological analytes. SERS amplification derives mainly from the electromagnetic interaction of light with metals, which produces large enhancement of the electromagnetic fields from a laser illumination source by exciting localized surface plasmon (LSP) resonance of nanoscale metal features.[1] Due to the ability of metal nanoparticles to concentrate electromagnetic fields within several nanometers of their surface, electrons associated with the high field region experience intense oscillation, resulting in generation of an elevated rate of Raman scattering events. SERS structures of this variety have included structures intentionally fabricated to include nanometer-scale points and tips for focusing electromagnetic energy into subdiffraction limited volumes.[2,3] Recently, several promising approaches for generating even greater SERS enhancements have taken advantage of the large electromagnetic fields that can be generated between adjacent metal regions separated by a dielectric gap (typically air) of 5–20 nm. The resulting electromagnetic "hot spots" have demonstrated peak SERS enhancement factors (EFs) as high as 10^8–10^{11}.[4–7] Recent reports have shown that a peak EF of 10^7–10^8 is sufficient for SERS detection of individual molecules.[8,9] However, while a high EF is obtained within the hot spot, the area density of hot spots may result in only a small fraction of the total surface area of a SERS substrate that is active. Experimentally measured ensemble-averaged SERS enhancements are 10^5–10^7 despite the presence of hot spots with substantially higher EF.[6,10–12]

A limitation that is preventing widespread adoption of the majority of SERS approaches is their fabrication by multistep microfabrication processes and/or low throughput and costly patterning approaches such as electron beam lithography or focused ion beam milling that are currently required to precisely define the nanostructure's size and shape.[5–7] For SERS to find widespread applications in routine chemical analysis, manufacturing process control, point-of-care diagnostics, and pharmaceutical research, the SERS device structure must be inexpensively manufacturable over large surface areas while providing a robust area-averaged enhancement factor. The glancing angle deposition (GLAD) technique has been demonstrated to be a simple, highly reproducible, and inexpensive method for fabrication of metallic nanostructures with high SERS enhancement factor due to its ability to produce randomly distributed nanoparticles with small gap size.[13] In this work, we use the GLAD technique to fabricate a high density coating of freestanding Ag nanoparticles that are supported vertically by SiO_2 dielectric post spacers over a silver-coated glass surface. Numerical simulations of the "post-cap" structure morphology are used to visualize the locations and overall density of hot spots under illumination by different excitation polarizations. Strong polarization dependence of SERS enhancement is demonstrated from both numerical simulation and measured SERS spectra. By altering the SiO_2 post spacer height, optimization of the interaction between the Ag nanoparticles and the underlying silver film can be achieved to maximize the local electric-field intensity and to increase the density of hot spots, leading to a maximum SERS EF of 2.38×10^9 within the hot spot region and a spatially averaged EF of 2.57×10^6.

Figure 1(a) schematically illustrates a cross section of the SERS substrate comprised of SiO_2–Ag "post-cap" nanostructures with an underlying continuous silver film (metal-SERS). To fabricate the Ag film, clean glass slide surfaces were precoated with a 200 nm silver thin film in an electron-beam evaporation system (Temescal). The GLAD technique was used to sequentially form both SiO_2 "post" and Ag "cap" nanostructures over large silver-coated surfaces in a single deposition run.[14] For comparison, the identical SiO_2–Ag "post-cap" nanostructures were also deposited onto an ordinary glass substrate without a silver film coating (glass-SERS). Figure 1(b) shows a cross-sectional scanning electron microscopy (SEM) image of SiO_2–Ag "post-cap" nanostructures with 20-nm-tall SiO_2 dielectric posts and freestanding Ag metallic caps with a height of 30 nm, fabricated upon a silicon substrate to facilitate imaging. Figure 1(c) presents the top-view SEM image of the fabricated metal-SERS substrate showing a high density coating of

a)Electronic mail: bcunning@illinois.edu.

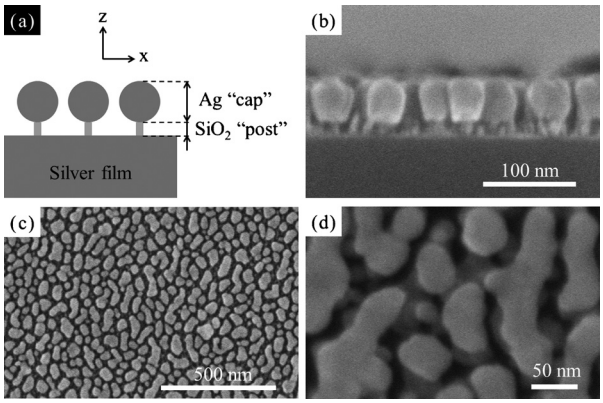

FIG. 1. (a) Schematic illustration (not to scale) of the cross section of the SiO_2–Ag "post-cap" nanostructures on silver thin film (metal-SERS). (b) Cross-sectional SEM image of SiO_2–Ag "post-cap" nanostructures on a silicon substrate. (c) Top-view SEM image of metal-SERS substrate. (d) Zoomed-in top-view SEM image of metal-SERS substrate.

electrically isolated Ag caps. A zoomed-in top-view SEM image shown in Fig. 1(d) indicates that the gap size between particles ranges from 5 to 20 nm. This image is also used as the two-dimensional geometry for electromagnetic simulation analysis.

To determine the near-field SERS gain at the surface of metallic nanoparticles, it is generally agreed that SERS enhancement (G_{SERS}) is proportional to the product of the local electric-field intensity enhancement at the incident laser and the Raman scattered wavelength when the electromagnetic models consider a molecule close to a metallic surface as a polarizable point dipole, which can be expressed as[15]

$$G_{SERS} \propto \left| \frac{E_{loc}(\lambda_{exc})}{E_{inc}(\lambda_{exc})} \right|^2 \left| \frac{E_{loc}(\lambda_{Raman})}{E_{inc}(\lambda_{Raman})} \right|^2,$$

where $E_{loc}(\lambda_{exc})$ and $E_{inc}(\lambda_{exc})$ are the local and the incident electric fields at the laser excitation wavelength, respectively. $E_{loc}(\lambda_{Raman})$ and $E_{inc}(\lambda_{Raman})$ represent the local and the incident electric fields, created and radiated by the analyte molecules close to a metallic surface, at the Raman scattered wavelength. In order to investigate the spatial distribution of G_{SERS} of our metal-SERS substrate, finite difference time domain (FDTD) method was used to study the spatial product of near-field intensity enhancements in response to normally incident plane waves from a HeNe laser ($\lambda = 632.8$ nm) and the Raman scattered wavelength ($\lambda = 692.5$ nm) corresponding to a Raman shift of 1363 cm^{-1} from the SEM image, as shown in Fig. 1(d).[14]

Figures 2(a) and 2(b) show the effects of incident light polarized along x and y axes on G_{SERS}, respectively. Simulated G_{SERS} maps indicate that the SERS intensity is maximized when the incident light is polarized along the x axis while minimized when polarized along the y axis. The observed polarization dependence occurs due to the self-shadowing effect of the GLAD process, in which individual nanoparticles are oriented mainly in the direction of the incoming flux of evaporated material, (i.e., y axis), resulting in a greater number of gaps along the x axis. Light polarized across these gaps can form hot spots, which are positioned at the gap edges where the greatest enhanced electric field is created. In our analysis, a hot spot is defined as the point where the spatial G_{SERS} value is larger than a G_{SERS} threshold (10^5), and the dimension of the hot spot is its spatial grid

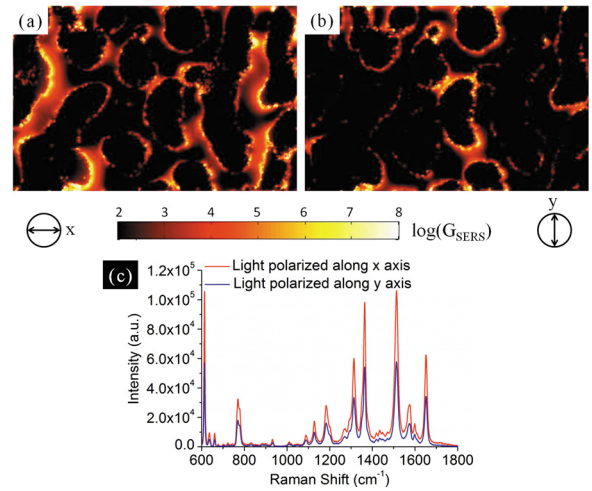

FIG. 2. (Color online) [(a) and (b)] Computer-simulated SERS enhancement maps of G_{SERS} for the SEM image shown in Fig. 1(d) for normally incident light polarized along x and y axes, respectively. (c) Correspondingly measured SERS spectra of 10 μM R6G on metal-SERS substrate.

volume (1 nm^3) around and within the gap. This thresholding enables a calculation of the number of hot spot "voxels" (i.e., volume pixels) in the entire simulation volume. In the following discussion, each voxel with $G_{SERS} \geq 10^5$ is counted as a single hot spot. The ratio of the numbers of hot spots for Fig. 2(a) compared to Fig. 2(b) is calculated to be ~3. The strong dependence on the polarization of the laser beam is also observed in the correspondingly measured SERS spectra of 10 μm Rhodamine 6G (R6G) on metal-SERS substrate shown in Fig. 2(c).[14] SERS intensities at 1363 cm^{-1} shift approximately increase by twofold when the laser beam's polarization is switched along the x axis. All SERS spectra and data reported below were the result of linearly polarized light along the x axis.

In order to examine the plasmonic coupling of the Ag caps and the silver film, the maximum G_{SERS} value and number of hot spots calculated from the 3D FDTD modeled metal-SERS map as a function of SiO_2 post thickness are shown in Fig. 3. It should be noted here that G_{SERS} and hot spots from those grid points located within the SiO_2 post

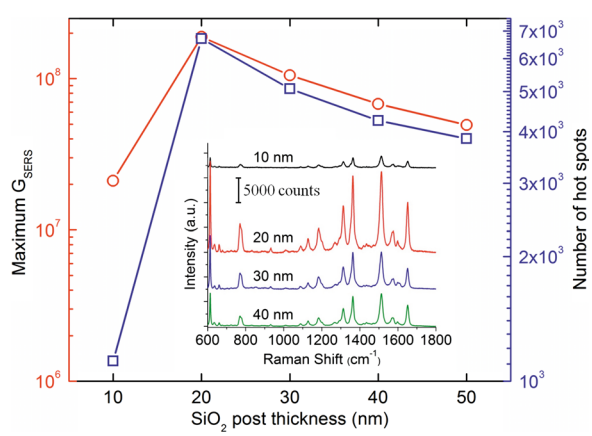

FIG. 3. (Color online) Plot of the maximum G_{SERS} (red circles, left axis) and the number of hot spots (blue squares, right axis) calculated from the 3D FDTD modeled metal-SERS G_{SERS} map as a function of SiO_2 post thickness for a fix Ag cap thickness of 30 nm. The inset shows SERS spectra of 1 μM R6G on metal-SERS substrates with different SiO_2 post thicknesses ranging from 10 to 40 nm for a fixed Ag cap thickness of 30 nm.

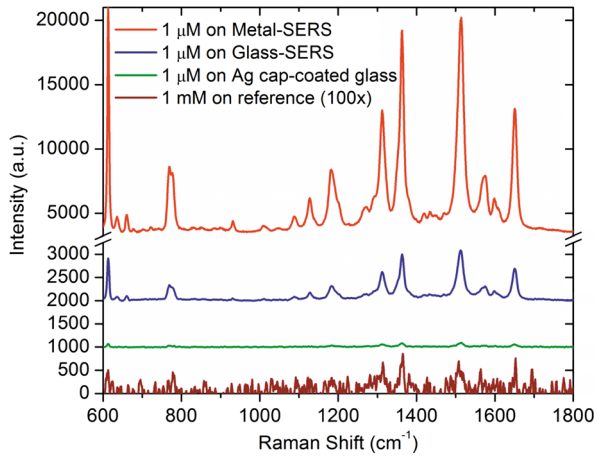

FIG. 4. (Color online) Comparison of SERS spectra of 1 μM R6G on metal-SERS, glass-SERS, Ag cap-coated glass substrates, and 1 mM R6G on reference sample without "post-cap" nanostructures (the reference spectrum was multiplied by a factor of 100 in the plot).

layer are not included in G_{SERS} and hot spot plots of Fig. 3, because analyte molecules cannot penetrate into the solid dielectric material and collective charge oscillations occur at a metal-dielectric interface. When the thickness of the SiO_2 post spacer is 10 nm, the most intense electric-field intensities are confined within the SiO_2 post layer, resulting in a dip in the maximum G_{SERS} plot and the low density of hot spots at the metal-dielectric interface. When the thickness of the SiO_2 post spacer is increased to 20 nm, both maximum G_{SERS} and the number of hot spots reach their maximum values, which can be attributed to a strong coupling between the LSPs on the Ag caps and the surface plasmon polaritons (SPPs) on the silver film.[16] This strong coupling leads to a sixfold increase in the number of hot spots relative to the structure with a 10-nm-thick SiO_2 post layer, because the most intense electric-field intensities concentrate within gaps rather than within the high refractive index SiO_2 post layer. Afterward, both maximum G_{SERS} and the number of hot spots decrease as the thickness of the SiO_2 post spacer is increased beyond 20 nm due to a weaker plasmon interaction effect. The inset in the figure presents the SERS spectra of 1 μM R6G on metal-SERS substrates with different SiO_2 post spacer thicknesses ranging from 10 to 40 nm for a fixed Ag cap thickness of 30 nm. Intensities of SERS spectra dependence on SiO_2 post spacer thickness show a very good agreement between the experimentally measured SERS spectra and the calculated number of hot spots.

For experimental verification of SERS performance of metal-SERS substrate, SERS spectra of 1 μM R6G on metal-SERS, glass-SERS substrates and an ordinary glass substrate directly deposited with 30 nm Ag caps without a SiO_2 post layer, and 1 mM R6G on an ordinary glass substrate coated with a 200 nm silver thin film as a reference were measured and compared, as shown in Fig. 4. Based on our previous method,[17] the experimentally measured average EF for glass-SERS substrate with a SiO_2 post thickness of 20 nm and Ag cap height of 30 nm was calculated to be 1.66×10^5 by using the intensity at 1363 cm^{-1} shift. This spatially averaged EF is mainly due to LSP hybridization of the dielectrically isolated Ag caps.[18] This SiO_2–Ag "post-cap" configuration provides approximately one order of magnitude greater SERS signal than the Ag cap-coated glass substrate (without posts) because a greater number of R6G molecules can occupy the volume surrounding the Ag on all sides. The SERS EF for metal-SERS substrate with the same "post-cap" nanostructure was calculated from experimental measurements shown in Fig. 4 to be 2.38×10^9 (Ref. 14) with a spatially averaged EF of 2.57×10^6. An additional 15-fold increase in the spatially averaged EF compared to the glass-SERS substrate can be attributed to the interaction between the LSPs on the Ag caps and their image charge on the underlying silver film.[15,19]

In conclusion, we have demonstrated that a SERS substrate comprised of SiO_2–Ag "post-cap" nanostructures with an underlying continuous silver film can be fabricated using a low-cost, large-area, and high-throughput GLAD technique. Both FDTD simulation results and experimentally measured SERS spectra confirm that the SERS enhancement is strongly polarization-dependent. Furthermore, by changing the thickness of the SiO_2 spacer sandwiched between the Ag caps and the silver film, strong coupling between LSP and SPP can be achieved to substantially enhance the near electric-field intensity and to increase the density of hot spots at the edge of the gaps. An experimentally measured SERS EF of 2.38×10^9 was obtained. The metal film/SiO_2 post/Ag cap structure provides a 180-fold increase in the spatially averaged EF relative to GLAD-deposited Ag caps on a glass substrate.

This work was supported by the National Science Foundation under Award No. CBET 07-54122 and ECCS 09-24062.

[1] K. A. Willets and R. P. Van Duyne, Annu. Rev. Phys. Chem. **58**, 267 (2007).
[2] J. A. Hutchison, S. P. Centeno, H. Odaka, H. Fukumura, J. Hofkens, and H. Uji-i, Nano Lett. **9**, 995 (2009).
[3] D.-K. Lim, K.-S. Jeon, H. M. Kim, J.-M. Nam, and Y. D. Suh, Nature Mater. **9**, 60 (2010).
[4] J. Theiss, P. Pavaskar, P. M. Echternach, R. E. Muller, and S. B. Cronin, Nano Lett. **10**, 2749 (2010).
[5] A. Gopinath, S. V. Boriskina, W. R. Premasiri, L. Ziegler, B. M. Reinhard, and L. D. Negro, Nano Lett. **9**, 3922 (2009).
[6] H. Im, K. C. Bantz, N. C. Lindquist, C. L. Haynes, and S.-H. Oh, Nano Lett. **10**, 2231 (2010).
[7] N. A. Hatab, C.-H. Hsueh, A. L. Gaddis, S. T. Retterer, J.-H. Li, G. Eres, Z. Zhang, and B. Gu, Nano Lett. **10**, 4952 (2010).
[8] P. G. Etchegoin and E. C. Le Ru, Phys. Chem. Chem. Phys. **10**, 6079 (2008).
[9] E. C. Le Ru, E. Blackie, M. Meyer, and P. G. Etchegoin, J. Phys. Chem. C **111**, 13794 (2007).
[10] L. Gunnarsson, E. J. Bjerneld, H. Xu, S. Petronis, B. Kasemo, and M. Käll, Appl. Phys. Lett. **78**, 802 (2001).
[11] Q. Yu, P. Guan, D. Qin, G. Golden, and P. M. Wallace, Nano Lett. **8**, 1923 (2008).
[12] Y. J. Liu, Z. Y. Zhang, Q. Zhao, and Y. P. Zhao, Appl. Phys. Lett. **93**, 173106 (2008).
[13] Seok-min Kim, W. Zhang, and B. T. Cunningham, Appl. Phys. Lett. **93**, 143112 (2008).
[14] See supplementary material at http://dx.doi.org/10.1063/1.3555342 for GLAD process, 3-D FDTD simulation, Raman instrumentation, SERS EF for metal-SERS substrate.
[15] N. Félidj, J. Aubard, G. Lévi, J. R. Krenn, A. Hohenau, G. Schider, A. Leitner, and F. R. Aussenegg, Appl. Phys. Lett. **82**, 3095 (2003).
[16] Y. Chu and K. B. Crozier, Opt. Lett. **34**, 244 (2009).
[17] C. J. Choi, Z. Xu, H.-Y. Wu, G. L. Liu, and B. T. Cunningham, Nanotechnology **21**, 415301 (2010).
[18] P. Nordlander, C. Oubre, E. Prodan, K. Li, and M. I. Stockman, Nano Lett. **4**, 899 (2004).
[19] P. Nordlander and E. Prodan, Nano Lett. **4**, 2209 (2004).